


ARTICLE

Reinforcement of Compressed Earth Bricks Using Locally-Sourced *Triumfetta pentandra* Fibers: Physical and Mechanical Evaluation

Roger Eno¹, Martial Ndé Ngnihameye², Emmanuel Foadieng³, Ekoum Ewandjo Nkoue¹, Fabien Kenmogne^{4*} , Rudy Kevin Tezempa Kouffeu⁵, Falonne Djofang Kongueb⁴, Moussa Sali⁶, Emmanuel Yamb Bell⁴, Sévérin Nguiya^{7,8}

¹ Laboratory for Mechanics and Materials (LMEMA), National Higher Polytechnic School of Douala, University of Douala, Douala P.O. Box 2701, Cameroon

² Department of Civil Engineering, National Advanced School of Public Works, Yaoundé 510, Cameroon

³ Department of Civil Engineering, Higher Technical Teacher Training College Kumba, University of Buea, Kumba P.O. Box 63, Cameroon

⁴ Department of Civil Engineering, Advanced Teacher Training College of the Technical Education, The University of Douala, Douala 1872, Cameroon

⁵ Department of Mechanical Engineering, Advanced Teacher Training College of the Technical Education, The University of Douala, Douala 1872, Cameroon

⁶ Laboratory of Materials, Mechanics and Civil Engineering, National Higher Polytechnic School of Maroua, University of Maroua, Maroua P. O. Box 46, Cameroon

⁷ Department of Common Trunk, National Higher Polytechnic School of Douala, University of Douala, Douala P. O. Box 2701, Cameroon

⁸ Laboratory for Geophysics (LG), National Higher Polytechnic School of Douala, University of Douala, Douala P. O. Box 2701, Cameroon

ABSTRACT

This study explores the novel application of *Triumfetta pentandra* (TP, “Nkui”) fibers, a tropical plant that is abundant

*CORRESPONDING AUTHOR:

Fabien Kenmogne, Department of Civil Engineering, Advanced Teacher Training College of the Technical Education, The University of Douala, Douala 1872, Cameroon; Email: kenfabien@yahoo.fr

ARTICLE INFO

Received: 1 September 2025 | Revised: 10 October 2025 | Accepted: 10 November 2025 | Published Online: 1 December 2025
DOI: <https://doi.org/10.30564/jbms.v7i4.11856>

CITATION

Eno, R., Ndé Ngnihameye, M., Foadieng, E., et al., 2025. Reinforcement of Compressed Earth Bricks Using Locally-Sourced *Triumfetta pentandra* Fibers: Physical and Mechanical Evaluation. *Journal of Building Material Science*. 7(4): 112–127. DOI: <https://doi.org/10.30564/jbms.v7i4.11856>

COPYRIGHT

Copyright © 2025 by the author(s). Published by Bilingual Publishing Group. This is an open access article under the Creative Commons Attribution-NonCommercial 4.0 International (CC BY-NC 4.0) License (<https://creativecommons.org/licenses/by-nc/4.0/>).

yet underutilized in civil engineering, to enhance the performance of compressed earth bricks (CEBs). The main objective is to assess how incorporating these vegetal fibers can improve the mechanical properties of CEBs while maintaining durability. TP fibers were extracted, characterized, and integrated into the soil used for brick specimens. A rigorous experimental protocol was implemented, featuring a unique fiber pre-treatment, the use of a single, homogeneous clayey soil type, and controlled 28-day curing under standard humidity and temperature, which distinguishes this study from previous works. Physical measurements (moisture content, bulk density, water absorption) and mechanical tests (fiber tensile strength, compressive and flexural strength of CEBs) were conducted following French standards. The results indicate that 4% TP fiber content yields optimal mechanical performance, with compressive strength reaching 6.61 MPa and flexural strength 1.49 MPa at 28 days, compared to 5.16 MPa and 0.51 MPa for unreinforced samples. This demonstrates the potential of TP fibers to reinforce earth-based materials, providing a sustainable, locally sourced, and cost-effective construction solution. However, higher fiber content increases porosity and capillary water absorption (up to 16.75 g at 6% fibers), highlighting the importance of optimized fiber dosing and potential complementary treatments for long-term durability.

Keywords: Compressed Earth Bricks; Triumphetta Pentandra Fibers; Physical and Mechanical Properties; Sustainability; Natural Fibers; Bio-Based Materials; Innovative Construction Materials

1. Introduction

Urban population growth continues to exert significant pressure on housing infrastructure. While this demand presents economic opportunities for the construction sector, it also brings into focus environmental sustainability challenges. The building industry, heavily reliant on materials like concrete and steel, faces criticism for its high environmental cost and misalignment with global sustainability goals^[1]. This has prompted a growing interest in eco-friendly, locally sourced alternatives. Among these alternatives, earth blocks (EB) have attracted attention due to their accessibility, low carbon footprint, and socio-economic advantages. When stabilized under optimal conditions, they offer effective thermal insulation and affordability^[2,3]. However, their mechanical weaknesses and poor water resistance require reinforcement through stabilizing agents^[4]. Traditionally, mineral binders such as lime and cement have been used for this purpose^[5]. Yet, their high carbon emissions contradict sustainability objectives.

Natural plant fibers have gained recognition as sustainable reinforcements capable of enhancing the mechanical properties of earth-based materials while promoting the use of local resources and supporting circular economies^[6-13]. Various fibers have been studied for their reinforcing potential. For example, Calamus rotang fibers have been shown to improve compressive strength up to 3.04 MPa after 28

days^[11], while coconut and date palm fibers increase mechanical performance up to an optimal concentration, beyond which structural benefits may decrease^[8,12]. Similarly, sugarcane bagasse and molasses positively affect ductility and compressive behavior^[6], and Pennisetum purpureum fibers exhibit tensile strength exceeding 1900 MPa, highlighting their potential for composite reinforcement^[13].

This study focuses on Triumphetta Pentandra (TP), a locally available and underutilized tropical plant whose fibers exhibit promising mechanical properties. Although TP fibers have been explored in polymer composites^[14], their application in compressed earth blocks (CEBs) remains largely unexplored. The selection of TP fibers is motivated by this research gap: despite being known in the literature, TP has not yet been tested for CEB reinforcement. Investigating this fiber provides novel insights and scientific value, offering a unique opportunity to enhance the performance of earthen materials. By evaluating the effects of TP fibers on CEBs, this research aims to contribute to sustainable, low-cost, and durable construction solutions. This study addresses the central research problem: Can earth blocks stabilized with TP fibers offer enhanced strength and durability, while remaining sustainable and locally adaptable? By investigating the physical and mechanical performance of CEBs reinforced with locally sourced Triumphetta pentandra fibers, this research contributes to sustainable construction practices, promotes the valorization of underutilized natural

resources, and aligns with climate-conscious development goals.

To systematically present this work, the article is structured in three main sections. The second section details the materials and methods, including the raw materials, fiber extraction process, soil characterization, preparation of compressed earth blocks (CEBs), and the laboratory tests used to assess their physical and mechanical properties. The third section presents and discusses the experimental results, covering moisture content, water absorption, density, tensile, compressive, and flexural strength, as well as bulk density and capillary water absorption, with an analysis of how TP fiber reinforcement affects block performance. Finally, the fourth section concludes the study by summarizing the key findings, highlighting the optimal fiber content for improved mechanical behavior, and providing recommendations for future research and sustainable construction applications.

2. Materials and Methods

The control of materials and experimental procedures is essential for investigating the physical and mechanical properties of CEB reinforced with TP fibers. This section describes the equipment, raw materials, and experimental techniques employed in this study. After fiber extraction, soil sampling, and earth block (EB) fabrication, a series of physical and mechanical characterizations were carried out, followed by laboratory tests designed to assess the performance of the produced CEBs.

2.1. Raw Materials

2.1.1. Soil

The soil used was collected from a site located near Bangangté, in the West Region of Cameroon (5°08'29" N, 10°31'18" E), as shown in **Figure 1**. Excavation was performed manually with a hoe and shovel down to a depth of 150 cm. The soil was then bagged in woven plastic sacks and transported to the laboratory (see **Figure 2**). In the laboratory, the samples were first dried in air for seven days to remove residual moisture. After drying, the soil was pulverized manually into a fine powder suitable for testing. This powdered soil served as the base material for the preparation of EBs^[15].

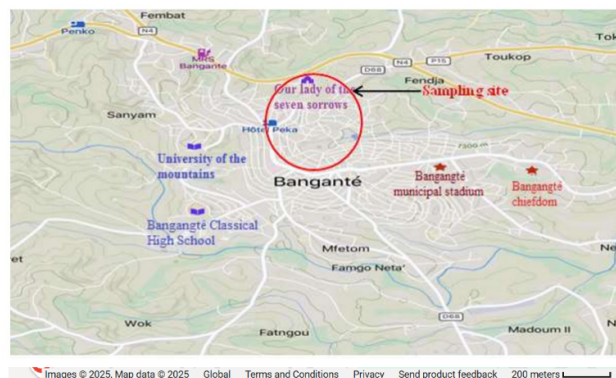


Figure 1. Geographic location of the sampling area.



Figure 2. Lateritic soil sample used for the study.

2.1.2. *Triumfetta Pentandra*

» Origin and Distribution

TP (locally called “Nkui”, see **Figure 3**) is widely distributed across tropical regions, from Cape Verde, Mauritania, and Senegal through Eritrea and Ethiopia, extending southwards to Namibia, Botswana, Zimbabwe, Mozambique, Madagascar, Réunion, and Mauritius. It grows from sea level up to 1700 m in gallery forests, woodlands, grasslands, wetlands, abandoned fields, and disturbed sites. In northern Cameroon, TP is sometimes considered an indicator of degraded soils^[14].



Figure 3. Stem of TP obtained in the west Region of Cameroon.

» Morphological Description

TP is an annual herbaceous plant that can reach 2 m in height. The stem is often woody at the base, succulent, reddish or green, and covered with stellate hairs. Leaves are alternate, simple, with triangular stipules (~7 mm), petioles up to 10 cm long, and laminae ranging from 1–12 cm × 0.5–9 cm. The leaf shape varies from elliptic to rhombic-orbicular, occasionally weakly lobed at the base. The lower surface bears stellate hairs and glandular structures^[16].

» Traditional and Potential Applications

In Cameroon, TP is widely used in the western region, particularly in the preparation of the traditional dish “Nkui”, reputed for its digestive, galactogenic, and anti-malarial

properties^[14]. According to the World Health Organization (WHO), phytotherapy remains widely practiced in developing countries. While the plant has received attention for food and medicinal applications, its fibers have largely been neglected and discarded as waste. Their valorization in CEBs therefore carries both environmental and economic significance.

» Fiber Sampling and Extraction

In this study, TP stems were collected in Bangoulap, a village located in the Ndé Division (West Cameroon). The geographical position of the site is shown in **Figure 4**. The region, part of the western highlands, was selected due to the availability and abundance of TP.



Figure 4. Process of fiber extraction from TP.

Fibers were extracted using cold-water retting, a technique reported in recent studies^[17]. Stems were cut into 30–40 cm pieces (**Figure 4a**) and submerged in containers of water at 25 ± 2 °C for 3–6 weeks (**Figure 4b**). During this period, microbial degradation softened the outer layers. Fibrous layers were then separated manually (**Figure 4c**), repeatedly washed with clean water (**Figure 4d**), and air-dried at ambient temperature (**Figure 4e**). Finally, the dried fibers were combed to obtain individual strands (**Figure 4f**).

2.2. Determination of Physical Properties

2.2.1. Moisture Content of TP Fibers

The moisture content of TP fibers was determined to quantify the amount of water present, expressed as a percentage of the wet sample mass. Following ISO 3344^[18], three fiber samples with an initial mass $m_1 = 1 \pm 0.1$ g were weighed on an analytical balance (sensitivity: 0.001 g). They were then oven-dried at 105 °C for 24 h, after which the final

mass was recorded. The moisture content was calculated using Equation (1):

$$H(\%) = \frac{(m_1 - m_2)}{m_1} \times 100 \quad (1)$$

where m_1 is the initial mass (g) of the wet sample and m_2 (g); the oven-dried mass.

The test was conducted at a room temperature of 27.6 °C.

2.2.2. Water Absorption Capacity of TP Fibers

The water absorption capacity of TP fibers was assessed using a gravimetric method^[19]. A total of 91 bundles, grouped into seven series, were tested. The procedure consisted of drying the samples in a Mermet oven at 105 °C for 1 h to remove residual moisture. The oven-dried mass of each sample (M_s) was measured with an analytical balance (precision: 0.001 g).

The dried fiber bundles were then tied with a string and attached to a small weight before being immersed in distilled water maintained at 28 °C for 24 h. After immersion, the samples were removed, lightly ventilated for 5 s to eliminate surface water, and reweighed to obtain the wet mass (M_h).

The water absorption rate (W(%)) was calculated according to Equation (2):

$$W(\%) = \frac{(M_{H24h} - M_s)}{M_s} \times 100 \quad (2)$$

where M_{H24h} is the mass of the fibers after 24 h immersion, and M_s the oven-dry mass.

The reported values correspond to the mean \pm standard deviation of the replicates.

2.2.3. Fiber Density

The density of TP fibers was determined by the pycnometer method using ethanol as the immersion liquid, in accordance with NF EN 1097-6^[15]. Ethanol was chosen due to its low surface tension and density of 0.789 g/cm³, which improves accuracy in porous materials.

The experimental procedure was as follows:

- The empty pycnometer was weighed to establish the tare mass.
- It was filled with ethanol up to the calibration mark, and the mass of ethanol alone (m_0) was determined.
- The fibers were weighed (m_1) and introduced into the pycnometer.

- The pycnometer was again filled with ethanol to the calibration mark and weighed, yielding a total mass $m_2 = m_1 + m_3$, where m_3 is the added ethanol mass. The fiber density was then computed using Equation (3):

$$\rho_{MP} = \frac{m_1}{m_0 - m_3} \times \rho_{ethanol} \quad (3)$$

where $\rho_{ethanol}$ is the density of ethanol. Four replicates were conducted, and the reported density corresponds to the arithmetic mean.

2.2.4. Natural Water Content of Soil

The natural water content, expressed as a percentage, of the soil was determined following NF EN ISO 17892-1^[18]. An empty container with lid was first weighed (m_1), then filled with a natural soil specimen and weighed again (m_2). The container, was placed in an oven for 24 h at 105 °C, after which the dried sample and container with lid were weighed (m_3). The water content (W) was calculated as:

$$W = \frac{(m_2 - m_3)}{m_3 - m_1} \times 100 \quad (4)$$

2.2.5. Atterberg Limits

The Atterberg limits (liquid limit W_L , plastic limit W_P , and plasticity index I_p) were determined in accordance with NF P 94-051 and NF P 94-052^[20]. These limits describe the transition of soil from liquid to plastic and from plastic to solid states.

- Liquid limit (W_L): determined using the Casagrande apparatus. A groove was carved in a soil paste placed in the cup, and the number of blows required to close the groove over 12 mm was recorded. The flow curve was established using four water contents corresponding to groove closure at 10, 20, 25, and 30 blows.
- Plastic limit (W_P): determined by rolling soil threads of 3 mm diameter on a glass plate until they crumbled. The corresponding water content was recorded.
- Plasticity index (I_p): calculated as:

$$I_p = W_L - W_P \quad (5)$$

The plasticity index classifies the soil according to its consistency and suitability for CEB production. Results were compared with the recommended plasticity chart. According to Cameroonian Standard NC 102–114^[18], soils that fall outside the recommended plasticity range may still yield

acceptable blocks in practice, although conforming soils generally provide more consistent results.

2.2.6. Standard Proctor Test

The compaction characteristics of the soil were determined using the Standard Proctor test (NF P 94-093)^[21]. The objective was to establish the maximum dry density and the corresponding optimum water content under a given compaction energy^[22]. Six samples of 2.5 kg each were prepared. Different amounts of water were gradually added and uniformly mixed by hand. The moistened soil was then compacted in three layers inside the Proctor mold, each layer being subjected to 25 blows with a standard rammer. After compaction, the specimens were demolded and weighed. Samples from the top, middle, and bottom were taken to determine water content after oven-drying at 105 °C. The procedure was repeated for all six samples with varying moisture contents. The results allowed plotting the compaction curve to determine the optimum moisture content and maximum dry density of the soil.

2.3. Mechanical characterization of the material (TP Fiber) and CEB

2.3.1. Mechanical Characterization by Tensile Test of the Fiber (NF EN 13895)

The tensile test is fundamental for determining the mechanical properties of the fibers, such as the elastic modulus, yield strength, tensile strength, and elongation at break. **Figure 5** shows a specimen mounted on the tensile testing device. Direct tensile tests on treated and untreated fibers from the pseudo-trunk of the oil palm were carried out using a universal testing machine, following the protocol of the NFT 25-501-2 standard^[23].

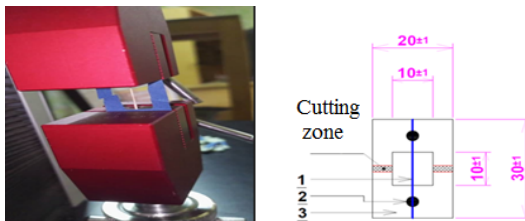


Figure 5. Tensile testing machine and specimen model.

- Fiber specimens were prepared with a gauge length (L_0) of 20 mm and tested at a constant speed of 5 mm/min at room temperature. Twenty specimens were tested for

each formulation, yielding a total of 260 samples. The tensile strength (σ (MPa)), the strain at break (ϵ), were obtained using Equation (6),

$$\sigma = \frac{F}{S}, \quad (6)$$

Where: F is the Force (N), S: the Cross-sectional area (mm^2), Δl : the Displacement (mm), and L_0 : the Gauge length (mm).

The Young's modulus was obtained using the least squares method applied to the linear portion of the stress-strain curve, consistent with Hooke's law ($y = ax + b$), where a represents the slope and corresponds to Young's modulus (MPa).

2.3.2. Formulation and Preparation of Specimens

Once collected, the soil was spread in thin layers and left to dry in open air for ten (10) days. It was then manually crushed and sieved through a 1.6 mm mesh.

The formulation of the material was carried out under the condition that optimal mixing was achieved with dry soil^[24,25]. Different mixtures were then prepared for block stabilization, using 600 g of soil in all cases, with varying proportions of TP fibers (0%, 2%, 4%, and 6%), while maintaining a constant water content. For each substitution rate, tests were conducted at curing ages of 7, 14, and 28 days. In every case, three specimens were tested, and the representative value was taken as the average of these three results. Water replacement was fixed at 12% across all formulations. The experimental program included compressive strength tests, three-point flexural strength tests, and porosity measurements. Overall, a minimum of $3 \times 3 \times 3 = 27$ specimens were tested for each substitution rate.

2.3.3. Manufacturing of Stabilized CEB (NF P 18-404)

»Preparation of Test Specimens

The specimens were prepared to ensure reliable evaluation of local materials. Standard molds of dimensions $4 \times 4 \times 16 \text{ cm}^3$ were used (see **Figure 6**)^[15]. While they are smaller than the full-scale bricks of 10–15 cm thickness, it has been widely observed that the mechanical performance trends obtained on smaller specimens are generally consistent with those expected for full-scale bricks. For the CEBs testing procedures, the manual^[26] suggests that laboratory specimens are often smaller than full-scale blocks, and that results can be extrapolated by considering scale effects and

adjusting for specimen geometry.

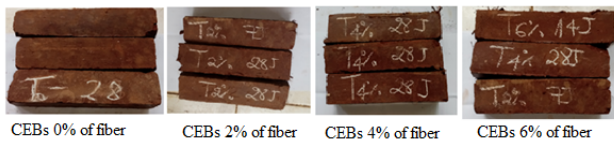


Figure 6. Compressed brick specimens ($4 \times 4 \times 16 \text{ cm}^3$) reinforced with TP fibers.

»Manufacturing Process

The tested samples were stabilized CEB reinforced with PT fibers. Fibers were added in dry condition at proportions of 0%, 2%, 4%, and 6% of the dry soil mass.

The manufacturing process involved several steps:

- Collection and preparation of raw materials.
- Mixing of soil, water, and fibers in a basin according to the proportions.
- Compaction of the mixture in a welded steel mold using a manually operated hydraulic press.
- Curing of the demolded blocks under ambient conditions.

The earth blocks were left to cure in open air for 7, 14, and 28 days before testing.

2.3.4. Compressive Strength of the Blocks

Compressive strength is defined as the ratio between the maximum load at failure and the cross-sectional area of the specimen. Tests were conducted according to the Cameroonian standard for CEB. Each specimen was placed between the plates of a compression testing machine and subjected to increasing loads until failure. The compressive strength was calculated using Equation (7):

$$\sigma_s = \frac{F}{S} \quad (7)$$

Where:

- σ_s : Compressive strength (MPa)
- F : Load at failure (N)
- $S = B \times H$: Cross-sectional area (mm^2), with $b = h = 40 \text{ mm}$

2.3.5. Flexural Strength

Flexural strength is defined as the maximum stress a material can withstand in bending before failure. The three-point bending test method was used using the equation:

$$\sigma = \frac{3Fd}{2le^2}, \quad (8)$$

where:

- σ = flexural strength (MPa),
- d = span between supports (50 mm),
- F = applied load on the specimen (N),
- L = specimen width (cm),
- e = specimen thickness (cm).

The specimen was placed on two parallel cylindrical supports, while a third cylindrical support, located at mid-span, applied the load through a hydraulic press. The apparatus consisted of a flexural testing machine and a caliper for dimensional measurements. Flexural strength was calculated using the standard bending stress relation^[15].

2.3.6. Capillary Water Absorption Test

After determining their dry mass (m_s), the blocks were partially immersed so that their bases were 5 mm above the water level. At predetermined intervals, the blocks were removed, surface-dried with a damp cloth, and weighed (m_h). This procedure was repeated for different immersion times. The test was performed in accordance with ASTM C20.

The water absorption coefficient (C_b) was calculated using Equation (9):

$$C_b = 100 \frac{(m_h - m_s)}{S\sqrt{t}} \quad (9)$$

This section presented the methodological steps adopted in this study. It first described the process of soil sample collection, followed by the preparation of the paste used for the fabrication of CEB specimens. Laboratory tests were then carried out in accordance with established standards and using appropriate equipment. Finally, the characterization and stabilization techniques applied to the collected samples were detailed to ensure the reliability of the results. These methodological foundations therefore provide a solid basis for the analysis and interpretation of the results to be presented in the following section.

3. Results and Discussion

This section presents and analyzes the results obtained from tests conducted on CEB reinforced with TP fibers. Observations focus on the physical and mechanical properties of the materials to evaluate their performance and compliance with expected technical standards. The objective is to interpret the collected data, identify significant trends, and discuss

the practical implications of the results, particularly in terms of durability, strength, and applicability in sustainable construction. This analysis allows for a better understanding of the actual impact of TP fibers on the blocks and highlights opportunities for improvement or future applications.

3.1. Physical Properties of Materials (TP Fibers and Soil)

3.1.1. Moisture Content of TP Fibers

The moisture content of TP fibers was determined on five samples collected from the bark of the stems (**Table A1**). These data were used to plot **Figure 7**.

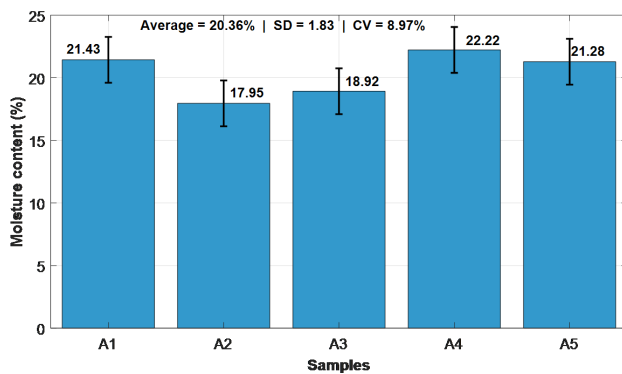


Figure 7. Variation of moisture content in TP fiber samples.

The average moisture content was 20.36%, higher than flax (10%), hemp (8%), and bagasse (8.8%)^[27], and also higher than TP fibers extracted by boiling water retting (11.23%)^[14]. This difference is likely due to the extraction method.

3.1.2. Water Absorption of TP Fibers

Water absorption was measured on five fiber samples (**Table A2**), resulting in **Figure 8**. The water absorption was 154.74%, indicating strong hydrophilicity, similar to sisal, flax, jute, and RC fibers. The hydrophilic character is attributed to hemicellulose and the lumen structure of the fibers. TP fibers absorb more water than pennisetum purpureum stems and roots (142.46%)^[11], but less than neupeltis acuminata (276.16%), Sida Rhombifolia (225.12%), or TP fibers extracted by hot-water retting (183.31%)^[14].

3.1.3. Density of TP Fibers

Fiber density was measured on four samples (**Table A3**) and is presented in **Figure 9**. Density ranged from 0.44

to 0.53 g/cm³, with a mean of 0.51 g/cm³, lower than Pennisetum Purpureum (1.35–1.34 g/cm³)^[11], but higher than TP fibers extracted by hot-water retting (0.351 g/cm³)^[14]. Due to their low density, TP fibers are suitable for composite or textile applications.

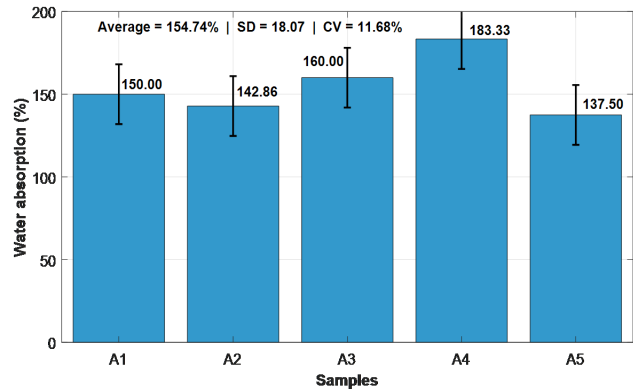


Figure 8. Water absorption of TP fibers.

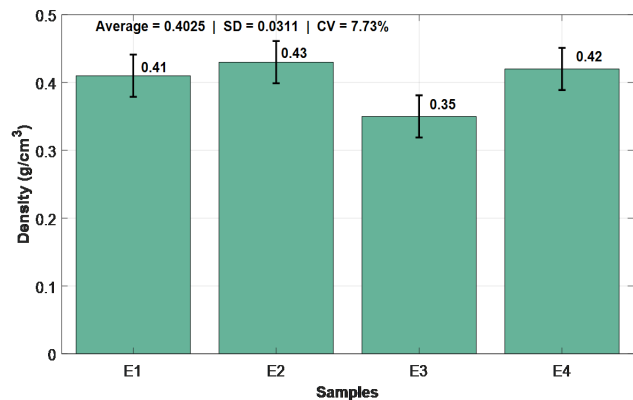


Figure 9. Density of TP fibers.

3.1.4. Natural Water Content of Soil

A wet soil mass of 200 g was oven-dried, yielding 175.698 g of dry soil. The natural water content W was calculated using Equation (2) to give $W=13.83\%$.

3.1.5. Atterberg Limits

Plasticity and liquid limit tests were performed as shown in **Table A4**. The liquid limit curve as a function of the logarithm of the number of blows is presented in **Figure 10**. The liquid limit corresponds to 25 blows. The plasticity index classifies the soil as moderately plastic (USCS), while the liquid limit indicates high cohesion. These results are slightly within the recommended ranges for CEB according to XP P 13-901.

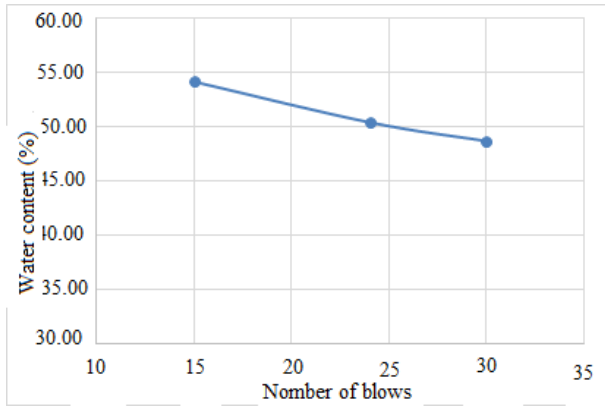


Figure 10. Liquid limit curve versus number of blows.

3.1.6. Standard Proctor Test

The results of the standard Proctor test are shown in **Table A5**. This test is performed under a layer-by-layer dynamic compaction scheme, which differs from the high-pressure pressing used for industrial CEB production. Consequently, the densities obtained from Proctor tests are highly dependent on the compaction energy and method applied^[22,28]. The curve of dry density versus water content is shown in **Figure 11**.

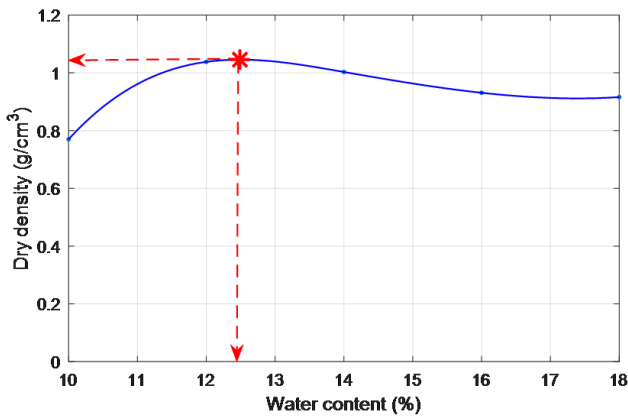


Figure 11. Dry density of soil versus water content.

The optimum moisture content corresponds to the tangent point on the curve: $W_{opt} = 12.4\%$, and the maximum dry density is $\rho = 1.04 \text{ g/cm}^3$. Compared to recommended CEB values^[29], the optimum moisture content is slightly higher, which may increase the risk of shrinkage during drying. The dry density is lower than standard CEB values, which justifies the use of fiber reinforcement to improve block performance.

Let us mention that the mineralogy and particle size distribution of the base soil strongly influence the measured

dry density. Soils with high porosity or clay content may exhibit lower Proctor densities while still producing satisfactory blocks after pressing or stabilization^[30]. Finally, fiber reinforcement tends to reduce apparent density while improving certain mechanical parameters, such as crack bridging, compressive strength, and flexural strength. This behavior is consistent with our experimental results^[31].

3.2. Mechanical Properties of Material (PP Fiber) and CEB

3.2.1. Fiber Tensile Test

The results of the tensile tests performed on 30 fiber samples are summarized in **Table A6**. **Figures 12a–c** illustrate the behavior of the fibers under tensile load and the effect of fiber diameter on tensile stress. The fibers have an average diameter of 5.449 mm, an average Young's modulus of 8.6 GPa, and an average elongation at break of 2%.

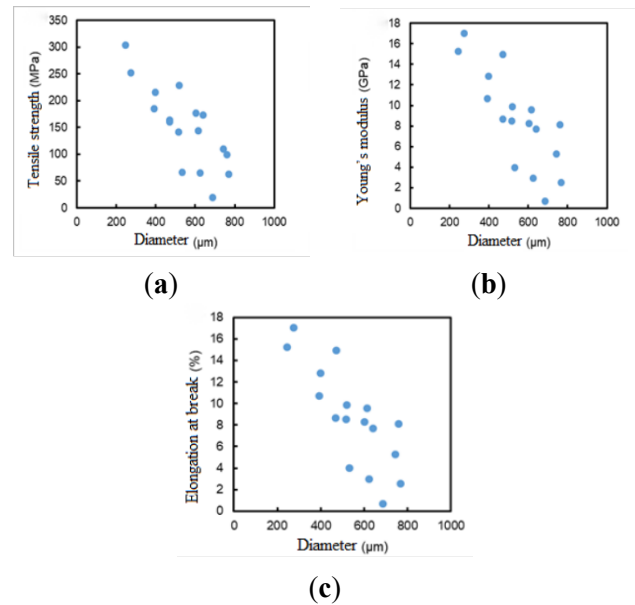


Figure 12. (a) Tensile strength vs diameter; (b) Young's modulus vs diameter; (c) Elongation at break vs diameter.

The graph in **Figure 13** shows the fiber stress-strain curve, from which the slope calculation shows that the fibers have an average modulus of elasticity of 8.6 GPa. Compared to other plants, these fibers have a higher elastic modulus than *Rachis* fibers (2.31 GPa), date palm fibers (2.5 GPa)^[32], and higher than the stem and root fibers of *Pennisetum Purpureum* (3.98 GPa and 1.55 GPa)^[11].

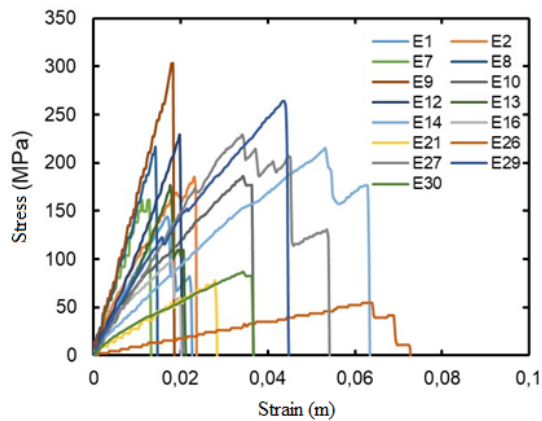


Figure 13. Stress-strain curves.

3.2.2. Compressive Strength of the Brick

Table A7 presents the compressive strength values of our bricks at 7, 14, and 28 days. These results allowed us to plot Figure 14. From the graph, we see that at 0% fiber, the strength of the stabilized CEB increases and reaches a maximum of 5.16 MPa after 28 days of curing. The same observation is made at 2%, 4%, and 6%, reaching maximum values of 5.21 MPa, 6.61 MPa, and 4.83 MPa after 28 days. At 7 days, the strength increases with fiber content and reaches a maximum (4.33 MPa) at 4% fibers, then decreases. The same pattern is observed at 14 and 28 days.

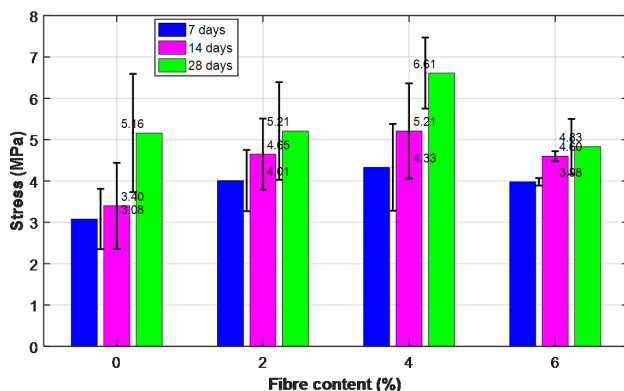


Figure 14. Compressive stress of CEB at 7, 14, and 28 days.

Thus, the stabilized CEB with 4% fiber addition exhibits satisfactory compressive performance, with strength increasing by approximately 28.10% compared to the 0% fiber case after 28 days. As the tests were conducted on a single, homogeneous soil type under controlled laboratory conditions, this observed increase to 28.10% can be reasonably attributed to fiber reinforcement rather than inherent soil variability. Comparable improvements have been

reported in the literature: Kumar et al.^[33] showed that reinforcement with *Pinus roxburghii* fibers led to similar gains in compressive strength of soil composites, while El-Emam and Al-Tamimi.^[34] observed that incorporation of natural palm tree fibers increased compressive strength by over 30% relative to unreinforced blocks. Furthermore, according to Le Troedec^[35], the typical compressive strength of standard CEBs ranges from 2 to 6 MPa. Therefore, the addition of 4% TP fibers not only enhances compressive performance but also ensures compliance with conventional construction standards.

3.2.3. Flexural Strength

Table A8 shows the flexural strength values at 7, 14, and 28 days, allowing the plotting of Figure 15. The CEB with 4% fiber shows optimal flexural performance, with a maximum flexural strength of 1.49 MPa at 28 days. The decrease beyond 4% may indicate reduced fiber-matrix bonding due to fiber overlapping^[36]. These values are higher than those reported by Kenmogne et al.^[11]: 0.6, 0.71, 0.64, and 0.62 MPa for 0%, 2%, 4%, and 6% fiber content, respectively.

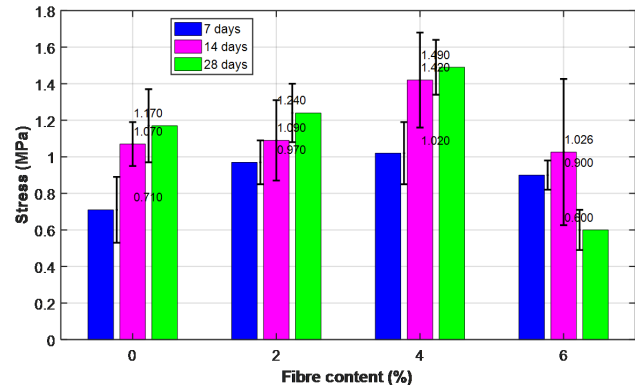


Figure 15. Flexural strength of CEB at 7, 14, and 28 days.

3.2.4. Bulk Density

To evaluate the effect of Calamus fiber on the physical properties of CEB, densities were measured for each specimen at 0, 7, and 28 days (Table A9). The graph of Figure 16 shows that density decreases with fiber addition, due to the density difference between fibers and soil. Density also decreases with drying time, as water content reduces, more so with higher fiber percentages. Maximum density: 2.12 g/cm³ at 0% (7 days); minimum: 1.71 g/cm³ at 6% (28 days).

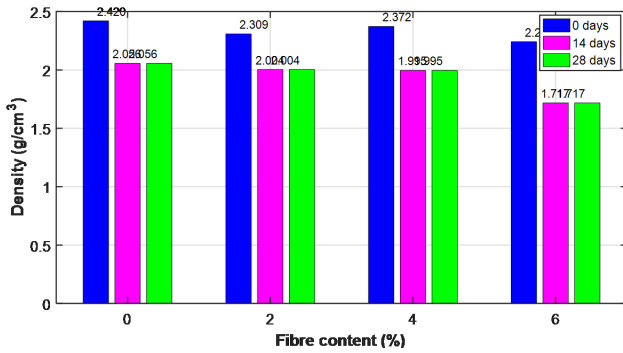


Figure 16. Bulk density of CEB at 0, 7, and 28 days.

3.2.5. Capillarity

Water absorption rates at 28 days are presented in **Table A10**, which allowed us to draw **Figure 17**. At 0% fiber, absorption increases until 20 s, decreases until 30 s, then rises to 10.90 g after 110 s. At 2%, maximum is 14.30 g; at 4%, maximum is 15.12 g; at 6%, maximum is 16.75 g. Water absorption increases with fiber content, likely due to the formation of interstitial voids^[37]. According to Djohore and Djomo^[38], the maximum absorption (8.51%) is below the 15% limit for vertical water penetration, confirming suitability for construction. This section presented the physical and mechanical test results of the studied materials. TP fibers demonstrated good moisture retention, high water absorption, and favorable mechanical properties, while the soil was suitable for CEB production. Fiber incorporation improved compressive and flexural strength, with optimal performance at 4%. Beyond this percentage, properties declined, likely due to reduced internal cohesion. The results confirm that fiber addition effectively strengthens bricks while remaining compliant with construction standards.

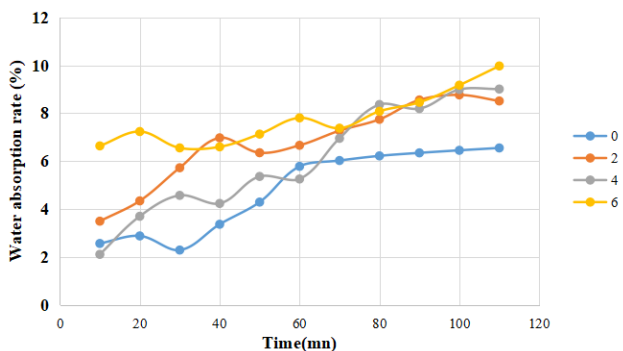


Figure 17. Water absorption rate of CEB.

4. Conclusions

This study contributes to the valorization of local natural resources by exploring the use of *Triumfetta pentandra* (TP) fibers as reinforcement for compressed earth blocks (CEBs), offering a sustainable and cost-effective solution for ecological construction in developing countries. A thorough experimental characterization of both the fibers and the CEBs was performed. TP fibers exhibited an average moisture content of 20.36%, water absorption of 154.74%, and a bulk density of 0.51 g/cm³, providing essential data to assess their influence on block performance. CEBs incorporating 0%, 2%, 4%, and 6% TP fibers were evaluated for mechanical and physical properties.

The results demonstrated that a 4% fiber content yielded the best overall performance. Compressive strength increased by 28.10% and flexural strength by 192.19% relative to unreinforced blocks, confirming the significant reinforcement potential of TP fibers. At the same time, increasing fiber content progressively reduced bulk density and increased capillary water absorption, reaching up to 16.75 g at 6% fiber content, indicating higher porosity that could affect durability under humid conditions. This highlights the need for careful optimization of fiber dosage to balance mechanical enhancement with physical stability. To mitigate the observed increase in water absorption and porosity, possible solutions include surface coatings or fiber pretreatments, which could protect the blocks and extend their service life. Furthermore, the manual mixing method employed may lead to fiber clustering, suggesting that improved mixing techniques or mechanized incorporation could enhance uniformity and consistency of reinforcement. Since the present experiments were already completed, no quantitative image analysis was conducted to verify fiber distribution. Future research will integrate this aspect by leveraging advanced computer vision techniques for more objective and accurate microstructural assessment. In particular, robust vision-based deep learning models, such as DeepLab^[39–41], could be applied to brick microstructure images to quantify fiber dispersion, porosity, and crack patterns with high precision.

To further advance this research and broaden its applications, the following perspectives are recommended:

- Assess the durability of TP fiber-reinforced CEB under real climatic conditions, including rainfall, humidity,

and temperature fluctuations;

- Investigate the effect of hydrophobic or protective treatments applied to TP fibers to reduce water sensitivity and improve longevity;
- Explore automated, computer vision-based methods for quantifying microstructural features, enabling more objective and scalable evaluation of reinforcement effects.

Author Contributions

All authors contributed equally to the conception, design, data collection, analysis, and writing of this study. All authors have read and agreed to the published version of the manuscript.

Funding

This work received no external funding.

Institutional Review Board Statement

Not applicable.

Informed Consent Statement

Not applicable.

Data Availability Statement

All data generated or analyzed during this study are included in this published article.

Conflicts of Interest

The authors declare no conflict of interest.

Appendix A

Table A1. Moisture content of TP fibers.

Samples	M _h (g)	M _s (g)	MC (%)
A1	0.34	0.28	21.43
A2	0.46	0.39	17.95
A3	0.44	0.37	18.92
A4	0.55	0.45	22.22
A5	0.57	0.47	21.28
Average			20.36
Standard Deviation			1.83
Cv			8.97

Table A2. Water absorption of TP fibers.

Samples	M _s (g)	M _h (g)	WA (%)
A1	0.08	0.2	150
A2	0.07	0.17	142.86
A3	0.1	0.26	160
A4	0.06	0.17	183.33
A5	0.08	0.19	137.5
Mean			154.74
Standard Deviation			18.07
Cv			11.68

Table A3. Density of TP fibers.

Samples	M0	M1	M2	ρ(g/cm ³)
E1	0.16	67.62	67.77	0.41
E2	0.17	67.58	67.73	0.43
E3	0.16	67.56	67.77	0.35
E4	0.17	67.58	67.73	0.42
Mean				0.4025
Standard Deviation				0.0311
Cv				7.73%

Table A4. Atterberg limits.

Test Number	Number of Shots	Tare Mass	M1 + Wet Tare (Mass of the Sample Taken after Carrying out the Test)	M2 + Dry Tare (Mass of the Sample after Passing through the Oven)	M1 Wet (Mass of the Sample Taken after Carrying out the Test)	M2 Dry (Mass of the Sample after Passing through the Oven)	Wi (Mass Water Content Which Corresponds to the Liquid or Plastic Limit for the Test)
Liquidity Limit							
30	15	111.4	132.16	124.87	20.76	13.47	54.12
31	24	67.98	92.4	84.22	24.42	16.24	50.37
32	30	111.21	132.51	125.54	21.3	14.33	48.64
w _l (Liquidity limit) %					51.04		
Plasticity Limit							
1	26A	68.16	73.5	72.15	5.34	3.99	33.83
2	37A	28.72	32.98	31.87	4.26	3.15	35.24
w _p (Plasticity limit(%))							34.54
Plasticity Index (Ip)(%)							16.5
Consistency Index (Ic)(%)							1.97

Table A5. Results of the Proctor test on soil.

Net Molding Weight (q)	6500		6500		6500		6500		6500	
Mixing Water (%)	10%		12%		14%		16%		18%	
Tare Weight No.	E1H	E1B	E2H	E2B	E3H	E3B	E4H	E4B	E5H	E5B
Total Wet Weight (g)	151.38	131.28	127.17	109.39	116.8	102.79	149.13	153.37	151.34	137.9
Total Dry Weight (g)	120.29	124.28	119.22	104.2	109.92	97.45	133.58	136.48	122.73	133.64
Tare Weight (g)	77.53	73.85	64.6	67.47	64.1	64.6	73.33	71.78	72.69	68.29
Water Weight (g)	31.09	7	7.95	5.19	6.88	5.34	15.55	16.89	28.61	4.26
Dry Material Weight (g)	42.76	50.43	54.62	36.73	45.82	32.85	60.25	64.7	50.04	65.35
Water Content (w) (%)	72.708	13.881	14.555	14.130	15.02	16.26	25.81	26.11	57.174	6.52
Average Water Content (%)	43.294		14.343		15.635		25.957		31.847	
Density Compaction Intensity (25 Strokes on 3 Layers)										
Mold No. H	15.6		15.6		15.6		15.6		15.6	
Total wet weight (g)	11100		11450		11340		11390		11540	
Mold weight (g)	6500		6500		6500		6500		6500	
Net wet weight (g)	4600		4950		4840		4890		5040	
Mold volume (cm^3)	4171.43		4171.43		4171.43		4171.43		4171.43	
Wet density (g/cm^3)	1.103		1.187		1.160		1.172		1.208	
Dry density (g/cm^3)	0.770		1.038		1.003		0.931		0.916	

Table A6. Summary of the desired tensile properties.

Sample	Diameter (μm)	Tensile Strength (MPa)	Young's Modulus (GPa)	Elongation at Break (%)
E1	614.8	143.9	9.5	1.7
E2	392.1	185.5	10.7	2.3
E5	624.2	65.7	2.9	2.4
E7	470.7	160.9	14.9	1.1
E8	398.8	216.2	12.8	1.4
E9	245.9	303.2	15.3	1.8
E10	515.7	141.7	8.5	2.4
E12	519.8	229.0	9.9	2.0
E13	602.9	176.5	8.3	1.8
E14	743.9	110.4	5.3	2.4
E16	759.8	98.8	8.1	1.8
E21	768.6	63.4	2.5	2.2
E23	275.3	251.9	17.0	1.4
E26	686.9	19.4	0.7	2.2
E27	640.7	173.1	7.7	2.3
E29	470.2	163.5	8.7	2.4
E30	532.9	66.4	4.0	2.4
Mean	544.9	151.2	8.6	2.0
Standard Deviation	157.9	75.1	4.6	0.4
Coefficient of Variation	29.0	49.7	53.8	

Table A7. Summary of CEB S compressive strengths and stresses.

7 Days						
Formulation	Strength (N) Ep1	Ep2	Ep3	Average	Stress (Mpa) σ_{comp}	Standard Deviation
0%	4548.84	6215.24	4008.38	4924.15	3.08	0.73
2%	6935.85	5066.78	7228.60	6410.41	4.01	0.74
4%	5945.02	9300.35	5517.16	6920.84	4.33	1.05
6%	6327.84	6530.51	6260.28	6372.88	3.98	0.09
14 Days						
0%	7408.75	4548.84	4368.69	5442.09	3.40	1.04
2%	9210.27	5854.94	7251.12	7438.78	4.65	0.86
4%	5809.90	9615.61	9593.09	8339.54	5.21	1.15
6%	7116.00	7588.90	7386.23	7363.71	4.60	0.12
28 Days						
0%	5404.56	8557.22	10809.12	8256.97	5.16	1.43
2%	8782.41	6305.32	9908.36	8332.03	5.21	1.18
4%	10133.55	12160.26	9457.98	10583.93	6.61	0.86
6%	6530.51	8106.84	8557.22	7731.52	4.83	0.67

Table A8. Summary of CEB S bending forces and stresses.

7 Days CEB S						
Formulation	Strength (N) EP1	EP2	EP3	Average	Stress (Mpa) σ_f	Standard Deviation
0%	195.09	251.29	204.78	217.06	0.71	0.18
2%	276.17	313.63	293.28	294.36	0.97	0.12
4%	312.02	292.32	334.63	312.99	1.02	0.17
6%	262.60	281.66	282.43	275.56	0.90	0.08
14 Days CEB S						
0%	304.59	314.60	356.59	325.26	1.07	0.12
2%	331.08	369.19	301.04	333.77	1.09	0.22
4%	469.64	424.10	408.27	434.00	1.42	0.26
6%	260.34	318.80	359.18	312.77	1.026	0.40
28 Days CEB S						
0%	306.85	329.46	429.59	355.3	1.17	0.20
2%	400.52	316.54	416.67	377.91	1.24	0.16
4%	455.43	426.36	478.04	453.28	1.49	0.15
6%	74.29	316.54	155.04	181.96	0.6	0.11

Table A9. Summary of CEB S densities.

Density at 0 Days			
Percentage of Fibers	Mass	Volume	Density (g/cm ³)
0%	692.31	286.08	2.42
2%	629.8767	272.85	2.3085
4%	636.1925	268.16	2.3724
6%	636.1925	283.84	2.2414
Density at 14 Days			
Percentage of Fibers	Mass	Volume	Density
0%	554.393	269.44	2.056
2%	558.793	278.827	2.004
4%	534.55	267.947	1.995
6%	434.447	253.013	1.717
Density at 28 Days			
Percentage of Fibers	Mass	Volume	Density
0%	554.393	269.44	2.056
2%	558.793	278.826	2.004
4%	534.55	267.947	1.995
6%	434.447	253.013	1.717

Table A10. Summary of the CEB absorption rate.

Dry Mass (g)				
	129.97	110.8	111.36	95.17
Mass of Water Absorbed (g)				
Time (s)	0%	2%	4%	6%
10	2.57	3.50	2.11	6.64
20	2.88	4.35	3.70	7.24
30	2.29	5.73	4.58	6.56
40	3.37	6.98	4.24	6.60
50	4.30	6.36	5.37	7.13
60	5.79	6.66	5.26	7.81
70	6.03	7.28	6.96	7.38
80	6.22	7.75	8.37	8.08
90	6.35	8.56	8.20	8.46
100	6.46	8.77	8.99	9.18
110	6.55	8.52	9.01	9.98

References

- [1] Taylor, M., Tam, C., Gielen, D., 2006. Energy efficiency and CO₂ emissions from the global cement industry. In Proceedings of the Energy efficiency and CO₂ emissions Reduction Potentials and Policies in the Cement Industry, Paris, France, 4–5 September 2006.
- [2] Turco, C., Mohammadmahdi, A., Elisabete, T., et al., 2024. Thermophysical properties of compressed earth blocks incorporating natural materials. *Energies*. 17(9), 2070. DOI: <https://doi.org/10.3390/en17092070>
- [3] Meukam, P., Noumowe, A., Jannot, Y., et al., 2003. Caractérisation thermophysique et mécanique de briques de terre stabilisées en vue de l'isolation thermique de bâtiment. *Materials and Structures*. 36, 453–460. DOI: <https://doi.org/10.1007/BF02481525>
- [4] Ashour, T., Hansjorg, W., Heiko, G., 2010. The influence of natural reinforcement fibers on insulation values of earth plaster for straw bale buildings. *Materials and Design*. 31(10), 4676–4685. DOI: <https://doi.org/10.1016/j.matdes.2010.05.026>
- [5] M'hamed Mahdad, A., Benidir, A., Brara, A., 2021. Experimental assessment of mechanical behavior of compressed stabilized earth blocks (CSEB) and walls. *Journal of Materials and Engineering Structures*. 8, 95–110.
- [6] Malanda, N., Louzolo-Kimbembe, P., Tamba-Nsemi, Y.D., 2017. Study of the mechanical characteristics of a clay brick stabilized with sugar cane molasses. *Revue RAMReS—Sciences Appliquées et de l'Ingénieur*. 2(2), 1–9. (in French)
- [7] Velasco-Aquino, A.A., Espuna-Mujica, J.A., Perez-Sanchez, J.F., et al., 2021. Compressed earth block reinforced with coconut fibers and stabilized with aloe vera and lime. *Journal of Engineering, Design and Technology*. 19(3), 795–807. DOI: <https://doi.org/10.1108/JEDT-02-2020-0055>

- [8] Kane, M.N., Ndiaye, M., Touré, P.M., et al., 2024. Physical and Thermo-Mechanical Properties of Composite Materials Based on Raw Earth and Crushed Palm Leaf Fibers (*Borassus aethiopum*). *Materials Sciences and Applications*. 15, 358–377. DOI: <https://doi.org/10.4236/msa.2024.159025>
- [9] Bobet, O., Nassio, S., Seynou, R., 2020. Characterization of peanut shells for their valorization in earth brick. *Journal of Minerals and Materials Characterization and Engineering*. 8(4), 301–315. Available from: <https://insa-toulouse.hal.science/hal-05030839v1>
- [10] Pacheco-Torgal, F., Said, J., 2011. Earth construction: lessons from the past for future eco-efficient construction. *Construction and Building Materials*. 29, 512–519. DOI: <https://doi.org/10.1016/j.conbuildmat.2011.10.054>
- [11] Kenmogne, F., Eno, R., Adile, A.D., et al., 2024. Comparative study of fibers extracted from the stems and roots of the Cameroonian *Pennisetum purpureum* for their applications in compressed earth brick reinforcement and textile engineering. *Materials Technology Reports*. 2(1), 1654. DOI: <https://doi.org/10.59400/mtr.v2i1.1654>
- [12] Enokela, O.S., Alada, P.O., 2012. Strength analysis of coconut fiber compressed earth for farm structures. *International Journal of Advancements in Research & Technology*. 1(2), 5–11.
- [13] Kenmogne, A.N., Ndoukouo, G.B., Ndombou, A., et al., 2025. Effects of waste fibers from *Calamus rotang* on the physical and mechanical characterizations of compressed earth blocks manufactured with the elastic soil of western region of Cameroon. *Journal of Modern Polymer Chemistry and Materials*. 4(1). DOI: <https://doi.org/10.53964/jmpcm.2025001>
- [14] Nkapleweh, A.D., Tendo, J.F., Ebanda, F.B., et al., 2022. Physico-chemical and mechanical characterization of *Triumfetta pentandra* bast fiber from the equatorial region of Cameroon as a potential reinforcement of polymer composites. *Journal of Natural Fibers*. 19(16), 13106–13119. DOI: <https://doi.org/10.1080/15440478.2022.2085228>
- [15] Gidigas, M.D., 1974. Degree of weathering in the identification of laterite materials for engineering purposes: a review. *Engineering Geology*. 8(3), 213–266. DOI: [https://doi.org/10.1016/0013-7952\(74\)90001-5](https://doi.org/10.1016/0013-7952(74)90001-5)
- [16] Burkill, H.M., 2000. *The Useful Plants of West Tropical Africa*, Vol. 5, 2nd ed. Royal Botanic Gardens: Kew, UK.
- [17] Ngoup, T., Efeze, N.D., Kanaa, T., et al., 2024. Physical, chemical and mechanical characterization of *Sida rhombifolia* fibers from the center region of Cameroon for their potential use in textiles and composites. *Journal of Natural Fibers*. 21(1). DOI: <https://doi.org/10.1080/15440478.2023.2294478>
- [18] Penka, J.B., Pettang Nana, U.J.M., Manjia, M.B., et al., 2022. Hydrological, mineralogical and geotechnical characterisation of soils from Douala (coastal, Cameroon): potential used in road construction. *Helvion*. 8(11), e11287. DOI: <https://doi.org/10.1016/j.helivion.2022.e11287>
- [19] Libog, L., Biyemea, F., Betené, A.D.O., et al., 2023. Influence of the extraction location on the physical and mechanical properties of the pseudo-trunk banana fibers. *Journal of Natural Fibers*. 20(2), 220–451. DOI: <https://doi.org/10.1080/15440478.2023.2204451>
- [20] Tchameni, A., Baud, P., Garnier, J.L., 2024. Improving soil dry compaction by adding granular material. In *Proceedings of the XVIII ECSMGE 2024 — European Conference on Soil Mechanics and Geotechnical Engineering*, Lisbon, Portugal, 26–30 August 2024; pp. 839–846.
- [21] Bouyila, S., Elenga, R.G., Ahouet, L., et al., 2019. NaOH activation of raw soils: effect of NaOH content on the drying kinetic and its modelling. *Geomaterials*. 9, 55–66. Available from: https://www.academia.edu/78780293/NaOH_Activation_of_Raw_Soils_Effect_of_NaOH_Content_on_the_Drying_Kinetic_and_Its_Modelling
- [22] Koadri, Z., Benyahia, A., Deghfel, N., 2019. Study of the effect of alkaline treatment time of palm fibers on the mechanical behavior of red clay-based materials from the M'sila region. *Matériaux et Techniques*. 107(4). DOI: <https://doi.org/10.1051/mattech/2019031> (in French)
- [23] Pickering, S.G., Efendy, N., Le, T.M., 2016. A review of recent developments in natural fibre composites and their mechanical performance. *Composites Part A: Applied Science and Manufacturing*. 83, 98–112.
- [24] Weyenberg, I.V., Truong, T.C., Vangrimde, B., 2006. Improving the properties of UD flax fibre reinforced composites by applying an alkaline fibre treatment. *Composites Part A: Applied Science and Manufacturing*. 37(9), 1368–1376. DOI: <https://doi.org/10.1016/j.compositesa.2005.08.016>
- [25] Guillaud, H., Doat, P., Rollet, P., 2008. *Earth Construction Technology and Architecture. Proposed Priority Research Directions for the Republic of Korea: Final Report (Volume 1/2)*. CRAtterre; Université Nationale de Mokpo; Chaire UNESCO Architecture de terre cultures constructives et développement durable: Grenoble, France. (in French)
- [26] Morel, J.-C., 2022. *Compressed Earth Blocks: Testing Procedures*. Centre for the Development of Enterprise (CDE): Brussels, Belgium.
- [27] Bledzki, A.K., Reihmane, S., Gassan, J., 1996. Properties and modification methods for vegetable fibers for natural fiber composites. *Journal of Applied Polymer Science*. 59(8), 1329–1336. DOI: [https://doi.org/10.1002/\(SICI\)1097-4628\(19960222\)59:8%3C1329::AID-APP17%3E3.0.CO;2-0](https://doi.org/10.1002/(SICI)1097-4628(19960222)59:8%3C1329::AID-APP17%3E3.0.CO;2-0)

- [28] Gilson, 2023. Proctor compaction test: A basic guide. Available from: <https://www.globalgilson.com/blog/proctor-compaction-test-a-basic-guide> (cited 9 July 2025).
- [29] Ngo'o Ze, A., Onana, V.L., Ndzié Mvindi, A.T., 2019. Variability of geotechnical parameters of lateritic gravels overlying contrasted metamorphic rocks in a tropical humid area (Cameroon): implications for road construction. *Bulletin of Engineering Geology and the Environment*. 78, 5531–5549.
- [30] Biwole, D., Fokwa, A.B., 2020. Effects of bamboo fiber length and content on the physicochemical and hygroscopic properties of compressed earth blocks used in construction. *Afrique Science*. 16(3), 161–171. Available from: <https://www.afriquescience.net/admin/postpdfs/9a6adac433c3eb2e4414efb98e01bfca1728668256.pdf> (in French)
- [31] Sadouri, R., Kebir, H., Benyoucef, M., 2024. The effect of incorporating Juncus fibers on the properties of compressed earth blocks stabilized with Portland Cement. *Applied Sciences*. 14(2), 815. DOI: <https://doi.org/10.3390/app14020815>
- [32] Sathishkumar, T., Navaneethakrishnan, P., Shankar, S., 2013. Characterization of natural fiber and composites: A review. *Journal of Reinforced Plastics and Composites*. 32(19), 1457–1476.
- [33] Kumar, R., Rakesh, P.K., Sreehari, D., 2022. Investigation on physico-chemical, mechanical and thermal properties of extracted novel pinus roxburghii fiber. *Journal of Natural Fibers*. 20(1). DOI: <https://doi.org/10.1080/15440478.2022.2157924>
- [34] El-Emam M., Al-Tamimi, A., 2022. Strength and Deformation Characteristics of Dune Sand Earth Blocks Reinforced with Natural and Polymeric Fibers, *Sustainability*. 14(8), 4850. DOI: <https://doi.org/10.3390/su14084850>
- [35] Le Troedec, M., 2009. Characterization of physico-chemical interactions in a composite material based on phyllosilicates, lime and cellulose fibers [PhD thesis]. Université de Limoges: Limoges, France. (in French)
- [36] Nkotto, L.I.N., Dounbissi Kamgang, G., Tiewa, J., 2020. Characterization of blocks produced by adding coconut fibers and laterite-cement based construction materials. *Afrique Science*. 17(4), 170–184. Available from: <https://www.afriquescience.net/admin/postpdfs/1b753aed4ecac0e94c7affaca16b6f8a1728410102.pdf> (in French)
- [37] Danso, H., Martinson, D.B., Ali, M., 2015. Physical, mechanical and durability properties of soil building blocks reinforced with natural fibres. *Construction and Building Materials*. 101(part 1), 797–809. DOI: <https://doi.org/10.1016/j.conbuildmat.2015.10.069>
- [38] Djohore, C.A., Djomo, S.A., 2018. Effect of adding potash-treated coconut fibers on the mechanical properties of clay-cement based construction materials. *European Scientific Journal*. 14(36), 104. DOI: <https://doi.org/10.19044/esj.2018.v14n36p104>
- [39] Baley, C., Le Duigou, A., Bourmaud, A., et al., 2012. Influence of drying on the mechanical behaviour of flax fibres and their unidirectional composites. *Composites Part A: Applied Science and Manufacturing*. 43(8), 1226–1233.
- [40] Song, Z., Zou, S., Zhou, W., et al., 2020. Clinically applicable histopathological diagnosis system for gastric cancer detection using deep learning. *Nature Communications*. 11, 4294. DOI: <https://doi.org/10.1038/s41467-020-18147-8>
- [41] Kabir, H., Wu, J., Dahal, S., et al., 2024. Automated estimation of cementitious sorptivity via computer vision. *Nature Communications*. 15, 9935. DOI: <https://doi.org/10.1038/s41467-024-53993-w>